Electronic Supplementary Material (ESI) for Chemical Communications

An oxidative coupling route to macrocyclic thiophenes and its application in the synthesis of a donor/acceptor hybrid molecule

Stefan K. Maier, Stefan-S. Jester, Ute Müller, Walter M. Müller, and Sigurd Höger*

Kekulé-Institut für Organische Chemie und Biochemie, Rheinische Friedrich-Wilhelms-Universität Bonn, Gerhard-Domagk-Str. 1, 53121 Bonn, Germany

E-mail: hoeger@uni-bonn.de (S. H.)

Supporting Information

Table of Contents

1 Experimental section

1.1 Materials and equipment

Reagents were purchased at reagent grade from commercial sources and used without further purification. All air-sensitive reactions were performed applying standard Schlenk techniques under Ar atmosphere and – if not otherwise indicated – using dry solvents (THF, CH_2Cl_2). The latter were dried, distilled and stored under Ar according to standard methods. Workup solvents were either used in "p.a." quality or purified by distillation. All solids and oils were dried overnight at r.t. under vacuum prior to characterization and further processing. ^{1}H and ^{13}C NMR spectra were recorded on Bruker AM 300, AM 400 and AM 500 spectrometers (300, 400 and 500 MHz for ^{1}H; 75.5, 100.6 and 125.8 MHz for ^{13}C). Chemical shifts are given in parts per million (ppm) referenced to residual ^{1}H or ^{13}C signals in $CDCl_3$ (^{1}H: 7.26, ^{13}C: 77.0), 1,1,2,2-tetrachloroethane-*d2* (^{1}H: 6.00, ^{13}C: 73.8) and *o*-dichlorobenzene-*d4* (^{1}H: 6.94, ^{13}C: 73.8). Deuterated solvents were obtained from Deutero GmbH, Germany. Mass spectra were measured on a Finnigan ThermoQuest MAT 95 XL (EI-MS), and a Bruker Daltronics autoflex TOF/TOF (MALDI-MS; matrix material: DCTB or dithranol, no salts added). MALDI HRMS data were recorded on a Bruker Daltonics Apex IV FT-ICR. Thin layer chromatography was performed on silica gel coated aluminium plates (Macherey-Nagel, Alugramm SIL G/UV_{254}, 0.2 mm silica gel coating with fluorescence indicator). Column chromatography was performed using silica gel 60 M (Macherey-Nagel, 40-63 μm) as stationary phase. Gel permeation chromatography (GPC) measurements were carried out by using an Agilent Technologies instrument with a set of 4 columns (PSS, polystyrene, 8 mm * 300 mm, 10^2, 10^3, 10^5 and 10^6 Å respectively) equipped with IsoPump G1310A, autosampler ALS G1329A, UV-detector VWD G1314B and refractive index (RI) detector RID G1362A, with THF (1 mL/min, HPLC grade, Fisher) as eluent. For the oligomer separation, a Shimadzu Recycling GPC (rec GPC) system, equipped with a LC-20 AD pump, a SPD-20 A UV detector and a set of three preparative columns from PSS (Polymer Standards Service, Mainz, Germany, 10^3 Å, 5 μ, 20 mm x 300 mm) was employed. The system was operated at a flow rate of 5 mL/min. Cyclic voltammetry was performed with a computer-controlled Model 602D Electrochemical Analyzer/Workstation of CH Instruments S3 with a glassy carbon disk (∅ = 1 mm) as working electrode on 0.2 mM solutions of molecules in dried and oxygen-free dichloromethane with 0.1 M tetrabutylammonium hexafluorophosphate (electrochemical grade, FLUKA) as supporting electrolyte, a platinum wire counter electrode, and a Ag/AgI

reference electrode (silver wire immersed in a Pyrex tube containing 0.2 M Bu_4NPF_6 + 0.02 M Bu_4NI in CH_2Cl_2) which was separated from the main solution by a ceramic frit. Redox potentials were referenced against ferrocene/ferrocenium (Fc/Fc+). HOMO/LUMO potentials were calculated using the absolute value of -4.8 eV to vacuum for the Fc/Fc+ redox potential.[1]

1.2 Scanning tunneling microscopy (STM)

Scanning tunneling microscopy (STM) measurements were performed under ambient conditions at the liquid/solid interface of a 10^{-5} M solution of the compound in 1,2,4-trichlorobenzene (TCB), and highly oriented pyrolytic graphite (HOPG). All samples were thermally annealed at 80 °C for ≤ 1 min and allowed to cool to r.t. prior to acquiring the images presented in this work. The experimental setup consists of an Agilent 5500 AFM/STM, placed on a Halcyonics active damping microscopy workstation encapsulated by a home-built acoustic isolation box. Mechanically cut Pt/Ir (80/20) tips were used and further modified *in situ* by applying short voltage pulses. Highly oriented pyrolytic graphite (HOPG) substrates were obtained from SPI Inc. in SPI-II quality and freshly cleaved before each experiment. Image processing was performed using the SPIP 5 (Image Metrology) software package. All molecular models shown are based on force-field geometry optimized backbone structures (with a graphene layer as interaction partner), using Spartan `08 (Wavefunction Inc.).

2 Additional STM images

Additional STM images of **10** at the TCB/HOPG interface are shown in Figures S1a and b, while Figure S1c is a reproduction of Figure 4a of the Main Text.

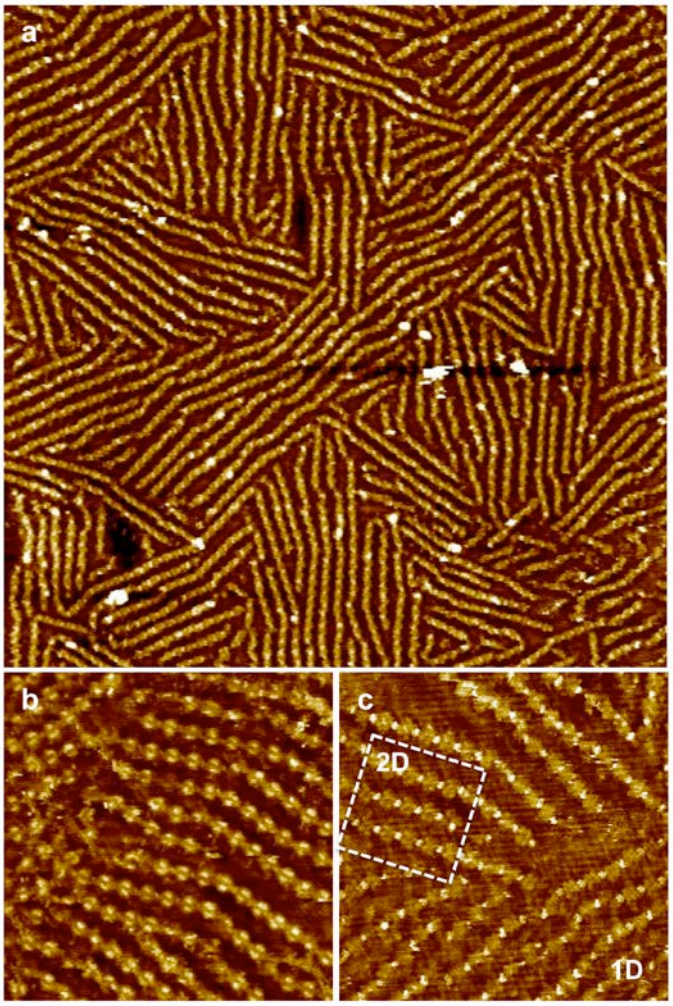

Figure S1: (a) – (c) STM images of 1D and 2D self-assembled **10** at the TCB/HOPG interface. In all cases, the molecular backbones are aligned in parallel to the substrate surface and assemble in (brightly appearing) lines of several 10 nm length that are separated by (darker) gaps covered by the alkoxy sidechains. (a) Overview image (200x200 nm^2, V_s = -1.1 V, I_t = 80 pA). The bright spots are attributed to impurities. (b) and (c) Small-area scans acquired at different bias voltages (b: 50x50 nm^2, V_s = -1.1 V, I_t = 30 pA; c: 50x50 nm^2, V_s = -0.7 V, I_t = 30 pA). The white dashed box in (c) indicates 2D self-assembly, whereas in the surrounding area of (c) only 1D self-assembly is observed (see text).

The rigid backbones of **10** assemble towards several ten nm long line-shaped structures, separated by regions covered with alkoxy sidechains. In all cases, a periodic pattern is observed along the line-shaped structures, representing individual molecules.

The conjugated aromatic backbones appear bright (indicating low tunneling resistance), while regions covered with the alkoxy sidechains are imaged as dark regions (denoting higher tunneling resistance).[2]

The STM image shown in Figure S1b was acquired at a sample bias voltage of -1.1 V leading to higher tunneling efficiency at the regions covered by the macrocyclic thiophene units of the backbones (as compared to the perylene bisimide units), so that circle-shaped structures are visible. Contrary, the image shown in Figure S1c was acquired at a sample bias voltage of -0.7 V, and a contrast inversion of the thiophene macrocycle and perylene bisimide moieties of each molecule is observed as compared to Figure S1b. The perylene bisimide units appear bright, while the macrocyclic parts of the molecules are only weakly resolvable. This behavior is assigned to the intermolecular combination of electron-rich and electron-poor units. Noteworthily, only one bright unit (instead of two units) is visible per molecule in Figure S1c. This behavior can be drawn back to stacking of the perylene bisimide units. Two perylene bisimide substituents of two adjacent molecules of a line pack onto each other and intermolecularly connect the backbones as displayed in Figure S2c, so that each bright spot in Figure S1c represents a dimer of two perylene bisimide units.

The box in Figure S1c indicates a region where 2D self-assembly is observed, best described by the molecular model shown in Figure S2a. A unit cell of a = 3.8 ± 0.3 nm, b = 3.2 ± 0.3 nm, and γ = 66 ± 3° is indexed. Only a part of the alkoxy sidechains is adsorbed to the substrate (along the HOPG main axis directions), and a line-to-line distance of w_{2D} = 3.5 ± 0.3 nm is observed. Contrary, the remaining part of Figure S1c is attributed to 1D ordering characterized by larger, variable line-to-line distances with a representative value of w_{1D} = 5.5 nm, as shown in Figure S2b. The adsorption of all alkoxy substituents (including the branched octyl parts of the 2-dodecyloctyloxy sidechains) would sterically frustrate the sidechain interdigitation, reducing the line-line interaction and thus the ordering from 2D to 1D. The limited interlocking of the molecules perpendicular to the line axes is in accordance with the observation of a less directional orientation of the lines (cf. bent 1D structures in Figure S1c, represented by the model Figure S2a).

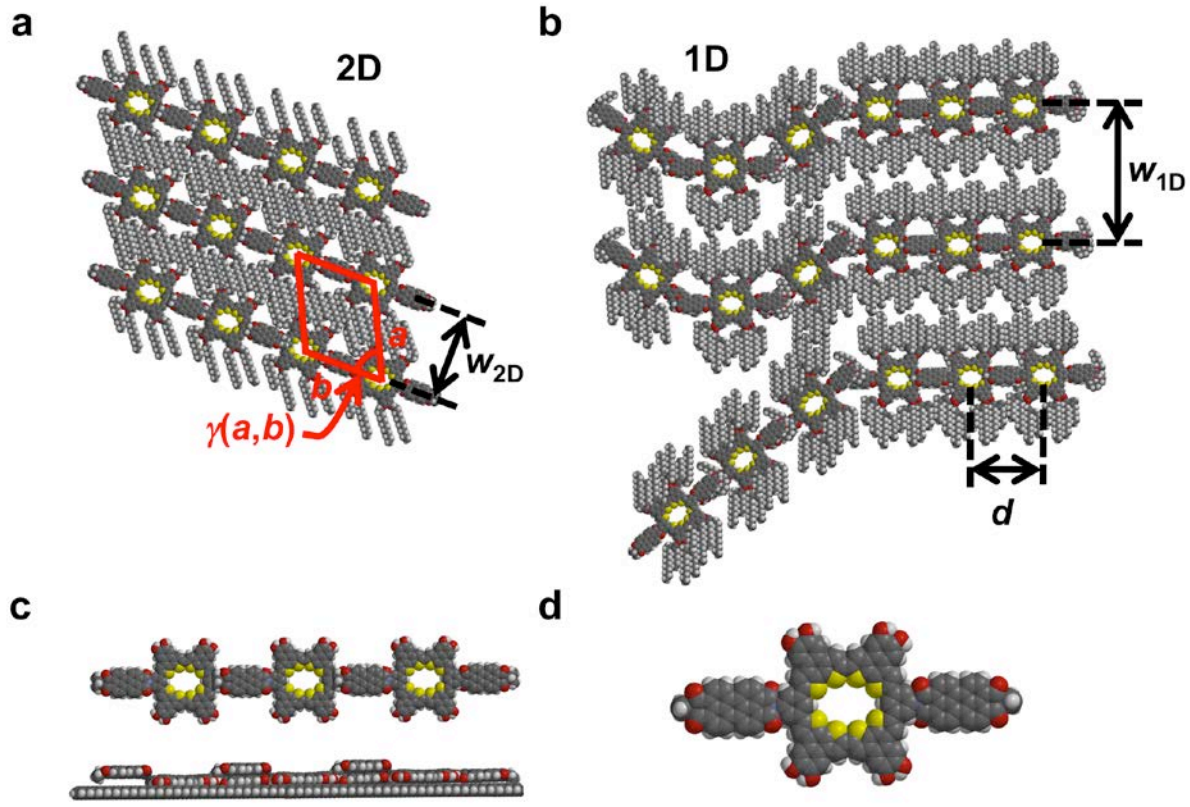

Figure S2: (a) – (b) Proposed structural models of **10** at the TCB/HOPG interface, consistent with the STM images observed in Figure S1. Two different patterns of self-assembly are observed. In both cases, (a) and (b), the molecules assemble into lines where two perylene bisimide units of two adjacent molecules point towards each other and are stacked, so that one stack of perylene bisimide units is observed per molecule (and appears bright in the STM image at the parameters chosen in Figure S1c). (a) 2D self-assembled monolayer with a = 3.8 ± 0.3 nm, b = 3.2 ± 0.3 nm, γ = 66 ± 3° (cf. dashed box in Figure S1c). Note that not all alkoxy chains, particularly not the -C_8H_{17} substituents of the branched sidechains, are adsorbed on the HOPG substrate, but point towards the solution phase and are not visible in the STM images (and not shown in the model). A minimum line distance of w_{2D} = 3.5 nm ± 0.3 nm is observed for the packing motif with interdigitating alkyl chains. (b) Representative model for the 1D self-assembly into chainlike structures, e.g. observed in the image part surrounding the dashed box in Figure S1c. From the line distance we conclude that all alkoxy substituents of the macrocyclic units (including branched parts) may be adsorbed on the HOPG substrate. The reduction from 2D to 1D ordering is drawn back to missing sidechain interaction. (c) Representation of three molecular backbones (neglecting the alkoxy sidechains) that visualizes the stacking of the perylene bisimide units. Top: top view; bottom: side view. (d) Rigid aromatic backbone of one molecule of **10**, consisting of the macrocyclic aromatic backbone and two perylene bisimide units.

3 Synthesis

2: To a solution of 461 mg (0.55 mmol) **1** in 6 mL dry chloroform and 4 mL glacial acetic acid 162 mg (0.72 mmol) *N*-Iodosuccinimide (NIS) were added in the dark and stirred overnight. The solvent was removed by distillation and the product was purified by column chromatography on silica gel using petroleum ether and dichloromethane (12:1) as eluent. The product was received as a colourless waxy solid (321 mg, 60 %).

^{1}H-NMR (500 MHz, $CDCl_3$, RT) δ [ppm]: 8.03 (s, 1H), 7.85 (d, *J* = 5.4 Hz, 1H), 7.62 (s, 1H), 7.54 (s, 1H), 7.47 (d, *J* = 5.3 Hz, 1H), 4.08-4.03 (m, 4H), 1.97-1.87 (m, 2H), 1.62-1.53 (m, 4H), 1.52-1.36 (m, 12H), 1.36-1.21 (m, 48H), 0.91-0.85 (m, 12H).

^{13}C-NMR (125 MHz, $CDCl_3$, RT) δ [ppm]: 149.5, 149.5, 135.2, 135.1, 133.9, 132.6, 129.0, 123.9, 122.6, 122.4, 121.3, 106.2, 106.0, 73.2, 71.8, 71.7, 38.2, 31.9, 31.5, 30.1, 29.8, 29.7, 29.7, 29.4, 29.4, 27.0, 22.7, 14.1.

MS (EI, 70 eV), m/z calcd for $C_{54}H_{87}IO_2S_2$: 958.5; found 958.4.

4: 210 mg (0.22 mmol) **2,** 41 mg (0.12 mmol) **3**, 37 mg (0.66 mmol) KOH and 6 mg (0.009 mmol) PEPPSI-IPr were dissolved in 5 mL THF (dry, degassed) and heated at 60 °C for 40 hours. After cooling to room temperature the mixture was diluted with dichloromethane, washed with saturated NH_4Cl-solution and water and then dried over $MgSO_4$. The product was purified by column chromatography on silica gel using petroleum ether and dichloromethane (5:1) as eluent. The product was received as a yellow solid (151 mg, 79 %).

^{1}H-NMR (300 MHz, $CDCl_3$, RT) δ [ppm]: 8.15 (s, 2H), 7.98-7.94 (m, 1H), 7.90 (d, *J* = 5.5 Hz, 2H), 7.73 (s, 2H), 7.68 (s, 2H), 7.64-7.62 (m, 2H), 7.49 (d, *J* = 5.3 Hz, 2H), 4.15 (d, *J* = 5.3 Hz, 4H), 4.08 (d, *J* = 5.5 Hz, 4H), 2.56 (s, 3H), 2.03-1.93 (m, 4H), 1.69-1.18 (m, 128H),, 0.92-0.82 (m, 24H).

^{13}C-NMR (75 MHz, $CDCl_3$, RT) δ [ppm]: 149.5, 149.4, 141.3, 139.4, 135.2, 134.7, 134.2, 130.0, 126.7, 123.6, 122.9, 122.7, 122.6, 121.6, 118.7, 106.5, 106.3, 71.8, 38.3, 38.2, 31.9, 31.5, 31.5, 30.2, 29.8, 29.8, 29.7, 29.4, 29.4, 27.1, 27.0, 22.7, 14.1.

MS (MALDI-pos, DCTB), m/z calcd for $C_{115}H_{180}O_4S_4$: 1753.3; found 1753.1.

5: 46.0 mg (0.026 mmol) of **4** dissolved in 30 mL dry $CHCl_3$ were slowly added to a stirred suspension of 150 mg (0.93 mmol) $FeCl_3$ (anhydrous) in dry $CHCl_3$ over 96 hours at room temperature. The black mixture was stirred for another 14 hours and was then poured into methanol. The yellow solution was washed four times with water, dried over $MgSO_4$ and filtered over silica gel using dichloromethane as eluent. The product was purified by rec GPC with THF as eluent to give 12.2 mg (27 %) of a dark yellow solid.

^{1}H-NMR (500 MHz, *o*-dichlorobenzene-*d4*, 373K) δ [ppm]: 8.38 (s, 2H), 8.04-7.99 (m, 8H), 7.83-7.80 (m, 8H), 7.61 (s, 4H), 4.32 (d, *J* = 5.5 Hz, 8H), 4.29 (d, *J* = 5.2 Hz, 8H), 2.51 (s, 6H), 2.14-2.04 (m, 8H), 1.86-1.74 (m, 16H), 1.74-1.20 (m, 240H), 0.94-0.83 (m, 48H).

^{13}C-NMR (125 MHz, *o*-dichlorobenzene-*d4*, 373K) δ [ppm]: 150.1, 150.0, 142.5, 139.3, 136.6, 135.4, 135.4, 134.9, 132.4, 130.1, 129.2, 126.9, 125.5, 123.8, 123.7, 123.5, 117.0, 107.9, 107.8, 72.7, 72.7, 38.9, 38.8, 31.9, 31.9, 31.8, 30.3, 30.2, 30.2, 29.8, 29.7, 29.6, 29.6, 29.3, 29.3, 27.3, 22.6, 22.5, 22.5, 21.5, 13.8, 13.7, 13.7.

MALDI HRMS, m/z calcd for $C_{230}H_{356}O_8S_8$: 3502.5211; found 3502.5192.

7: 1.32 g (2.3 mmol) **6** and 2.76 g (8.0 mmol) 3,5-diiodoaniline were dissolved in 40 mL *m*-cresol and 4 mL isoquinoline. The mixture was stirred for 1 hour at 80 °C, 2 hours at 120 °C, 2 hours at 140 °C and 4 hours at 200 °C. The warm mixture was poured into 250 mL acetone, stirred for 30 min, filtered and washed with water and 10 % NaOH solution. The red solid was dried in vacuum (1.68 g, 81 %).

^{1}H-NMR (300 MHz, $CDCl_3$, RT) δ [ppm]: 8.76-8.63 (m, 8H), 8.21-8.18 (m, 1H), 7.71-7.68 (m, 2H), 5.24-5.12 (m, 1H), 2.34-2.16 (m, 2H), 1.97-1.80 (m, 2H), 1.44-1.06 (m, 16H), 0.83 (t, *J* = 6.5 Hz, 6H).

MS (EI, 70 eV), m/z calcd for $C_{43}H_{38}I_2N_2O_4$: 900.1; found 900.2.

8: 450 mg (0.5 mmol) **7**, 508 mg (2.0 mmol) Bis(pinacolato)diboron $(Bpin)_2$, 294 mg (3.0 mmol) KOAc and 25 mg (0.03 mmol) $PdCl_2$(dppf) were suspended in 10 mL dry DMF and stirred for 15 hours at 60 °C. After cooling to room temperature the mixture was diluted with dichloromethane and washed twice with water. The product was purified by column chromatography on silica gel using cyclohexane, dichloromethane and ethylacetate (3:1:1) as eluent. The product was received as a red solid (379 mg, 84 %).

^{1}H-NMR (400 MHz, $CDCl_3$, RT) δ [ppm]: 8.77-8.63 (m, 8H), 8.41 (t, *J* = 1.0 Hz, 1H), 7.88 (d, *J* = 1.1 Hz, 2H), 5.24-5.15 (m, 1H), 2.35-2.18 (m, 2H), 1.93-1.82 (m, 2H), 1.33 (s, 24H), 1.28-1.20 (m, 16H), 0.83 (t, *J* = 6.9 Hz, 6H).

^{13}C-NMR (75 MHz, $CDCl_3$, RT) δ [ppm]: 163.6, 141.7, 137.5, 135.1, 134.5, 134.2, 131.9, 131.8, 131.2, 130.1, 129.8, 129.6, 126.7, 126.5, 124.1, 123.3, 123.3, 123.1, 83.9, 54.8, 32.4, 31.7, 29.2, 26.9, 25.0, 24.9, 22.6, 14.0.

MS (EI, 70 eV), m/z calcd for $C_{55}H_{62}B_2N_2O_8$: 900.5; found 900.4.

9: 88 mg (0.11 mmol) **8**, 192 mg (0.20 mmol) **9,** 34 mg (0.61 mmol) KOH and 6 mg (0.009 mmol) PEPPSI-IPr were dissolved in 5 mL THF (dry, degassed) and stirred at 60 °C for 42 hours. After cooling to room temperature the mixture was diluted with dichloromethane, washed with saturated NH_4Cl-solution, brine and water and then dried over $MgSO_4$. The product was purified by column chromatography on silica gel using petroleum ether and dichloromethane (3:2) as eluent. The product was received as a red solid (128 mg, 55 %).

^{1}H-NMR (500 MHz, 1,1,2,2-tetrachloroethane-*d2*, 373 K) δ [ppm]: 8.77 (d, *J* = 7.9 Hz, 2H), 8.65 (d, *J* = 7.9 Hz, 2H), 8.61-8.51 (m, 4H), 8.16 (s, 2H), 8.08 (s, 1H), 7.87 (d, *J* = 4.9 Hz, 2H), 7.83 (s, 2H), 7.73 (s, 2H), 7.66 (s, 2H), 7.52 (d, *J* = 5.1 Hz, 2H), 5.22 (s, 1H), 4.14 (d, *J* = 5.3 Hz, 4H), 4.07 (d, *J* = 5.4 Hz, 4H), 2.37-2.26 (m, 2H), 2.07-1.97 (m, 2H), 1.97-1.88 (m, 4H), 1.68-1.21 (m, 145H), 0.99-0.85 (m, 30H).

^{13}C-NMR (125 MHz, $CDCl_3$, RT) δ [ppm]: 163.1, 149.9, 149.8, 139.8, 136.5, 136.4, 135.1, 134.6, 134.3, 133.8, 131.6, 131.0, 130.9, 130.4, 129.9, 129.6, 129.2, 126.4, 126.1, 125.8, 124.0, 123.7, 123.0, 122.9, 122.8, 122.7, 122.5, 119.6, 107.4, 73.8, 72.6, 54.9, 38.5, 38.3, 32.4, 31.7, 31.7, 31.6, 31.5, 31.5, 29.9, 29.9, 29.5, 29.4, 29.4, 29.4, 29.3, 29.1, 29.1, 29.0, 28.0, 29.0, 26.9, 26.9, 22.4, 22.4, 22.3, 13.7, 13.7, 13.7.

MS (MALDI-pos, DCTB), m/z calcd for $C_{151}H_{212}N_2O_8S_4$: 2309.5; found 2309.5.

10: 15.0 mg (0.007 mmol) of **9** dissolved in 20 mL dry $CHCl_3$ were slowly added to a stirred suspension of 53 mg (0.33 mmol) $FeCl_3$ (anhydrous) in dry $CHCl_3$ over 96 hours at room temperature. The dark violet mixture was stirred for another 20 hours and was then poured into methanol. The red solution was washed with NH_4OH and NH_4Cl (aq) and dried over $MgSO_4$. The mixture was filtered over silica gel using chloroform as eluent. The product was purified by rec GPC with THF as eluent to give 3.5 mg (23 %) of a red solid.

GPC data and mass spectrum are displayed on p. S12.

4 Analytical data

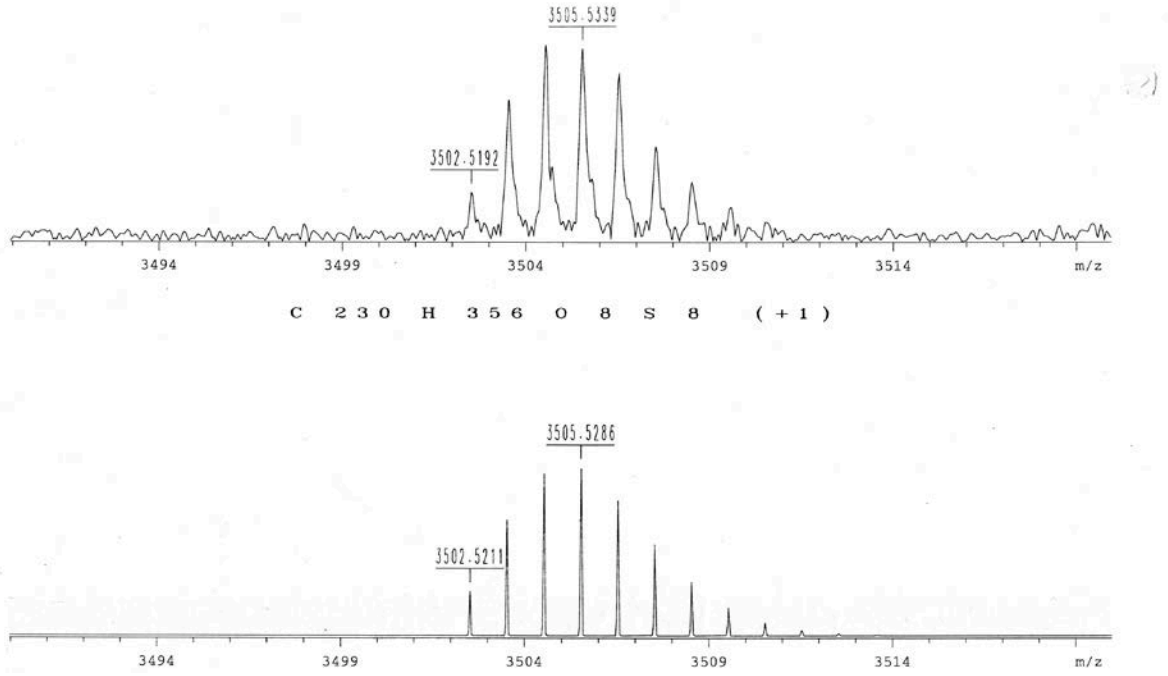

Figure S3: High-resolution MALDI mass spectrum of **5**, measured (on top) and calculated (bottom).

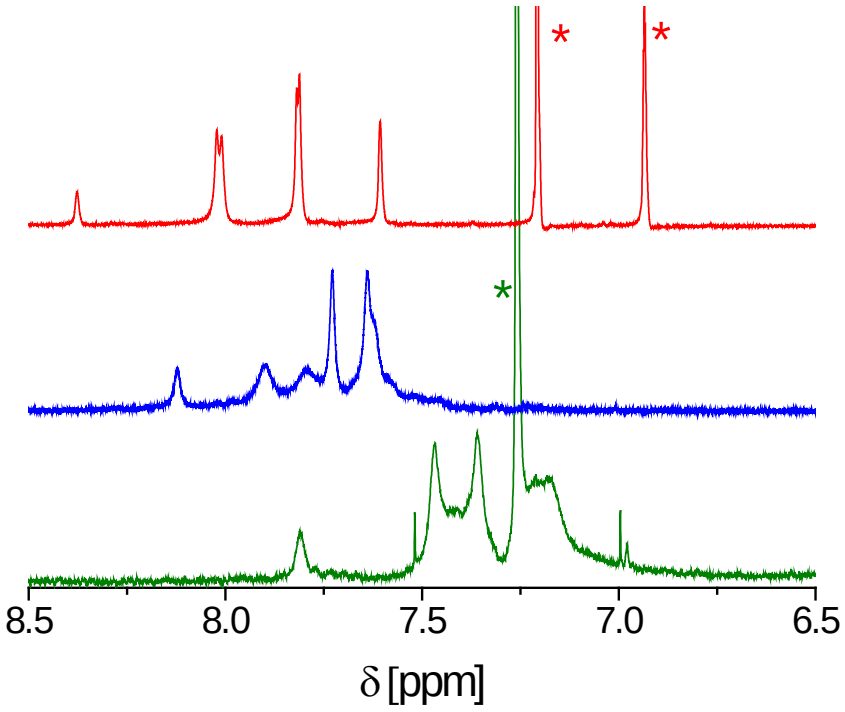

Figure S4: Aromatic region of the NMR spectra of **5** at room temperature in $CDCl_3$ (green), 373 K in tetrachloroethane-*d2*, and 373 K in dichlorobenzene-*d4*. Solvent signals are marked with an asterisk.

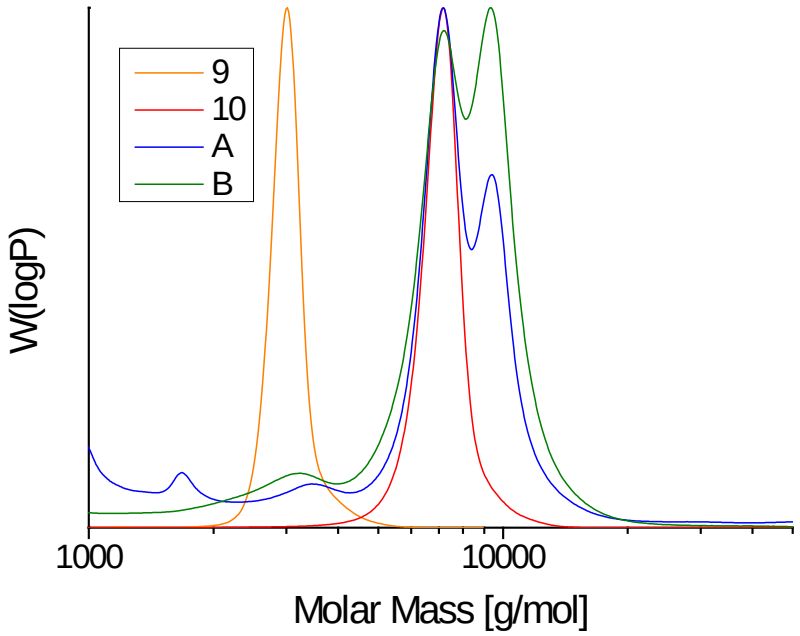

Figure S5: GPC data of **9** (orange), **10** (red) after rec GPC separation as well as **A** (blue) the soluble part of the crude product of **10** (insoluble red solid was removed by filtration through a syringe filter before the measurement) prepared as described on p. S10. **B** is the soluble part of the crude product of **10** prepared under different reaction conditions (26.0 mg **9** in 20 mL $CHCl_3$ was added to 50 mg $FeCl_3$ in 40 mL $CHCl_3$) to yield 3.5 mg (13 %) **10** after purification.

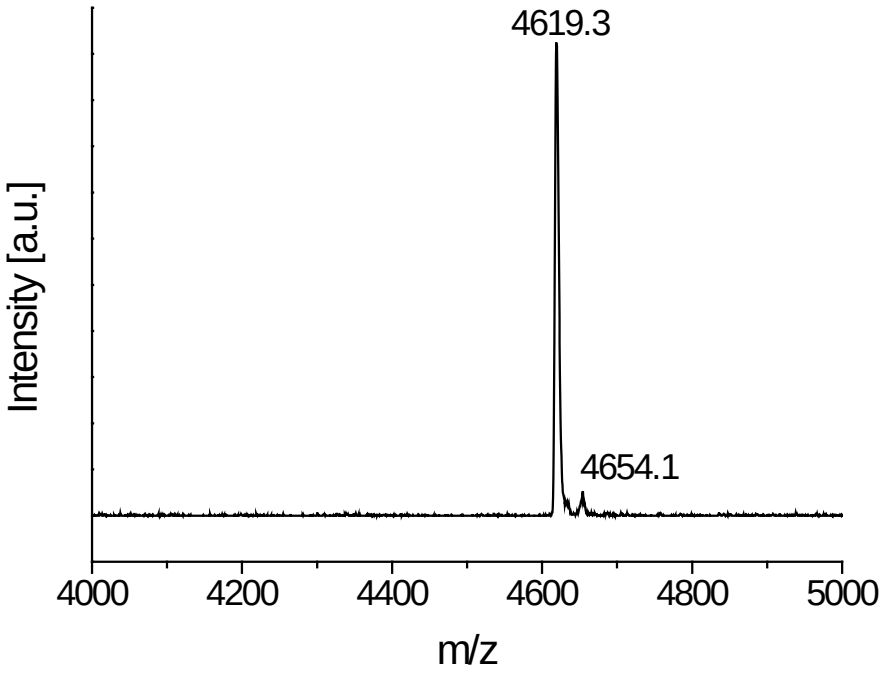

Figure S6: MALDI mass spectrum (dithranol matrix) of **10** (molar mass is 4619.1 g/mol). It was not possible to resolve the isotope pattern. The signal at 4654 Da indicates a small amount of chlorinated product that could not be removed.

5 References

[1] Pommerehne, J.; Vestweber, H.; Guss, W.; Mahrt, R. F.; Bassler, H.; Porsch, M.; Daub, J. *Adv. Mater.* **1995**, *7*, 551.

[2] For theoretical descriptions of the contrast mechanism in STM see, e.g.: a) Lazzaroni, R.; Calderone, A.; Brédas, J. L.; Rabe, J. P. *J. Chem. Phys.* **1997**, *107*, 99; b) Sautet, P. *Chem. Rev.* **1997**, *97*, 1097.